



Fock-Darwin States for an Elliptical Spin-Orbit Coupled Quantum Well

Marieke van Beest

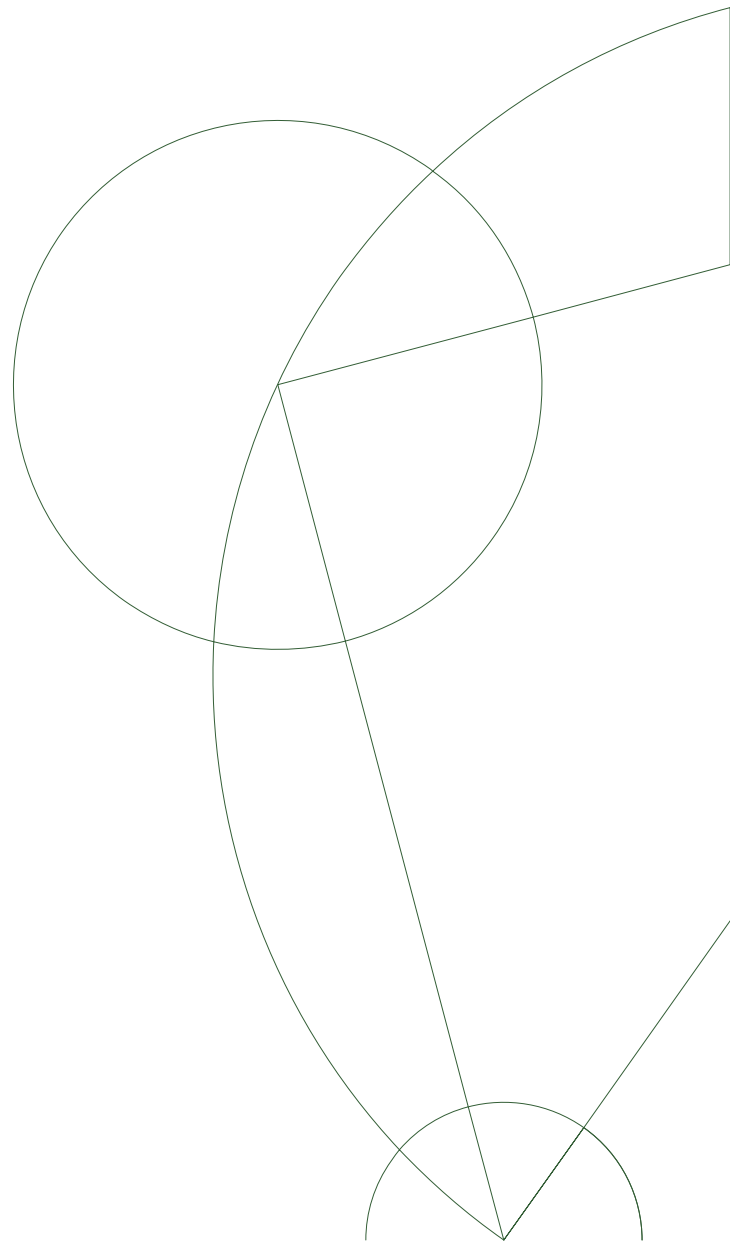
Bachelor's thesis in Physics

Advisor: Jens Paaske

Niels Bohr Institute

University of Copenhagen

Date: November 24, 2015



Abstract

Analytical solutions are derived for the wave functions and energy levels of an electron on a two-dimensional surface with a uniform magnetic field applied perpendicular to its plane of motion. A confinement potential in the form of an isotropic parabolic quantum well is imposed also on the electron moving in two dimensions in a magnetic field, and analytical solutions for the new wave functions and energy levels are obtained. The system is solved also for the general case of an elliptical confinement potential. The electron spin is then taken into consideration, specifically, we regard the Zeeman effect and Rashba spin-orbit coupling and the new energy levels are found numerically.

Contents

1	Introduction	1
2	Free Electron in a Uniform Magnetic Field	1
3	Fock-Darwin States for a Circular Quantum Well	3
3.1	Properties of Fock-Darwin States for a Circular Quantum Well	6
4	Fock-Darwin States for an Elliptical Quantum Well	9
4.1	Properties of Fock-Darwin States for an Elliptical Quantum Well	14
5	Spin	16
5.1	Zeeman Effect	16
5.2	Rashba Spin-Orbit Coupling	16
6	Conclusion	19
7	References	20
	Appendices	21
A	Transformation of Variables for an Elliptical Quantum Well	21
B	Finite Hamiltonian Matrix with Zeeman Effect and SO Coupling	22
C	Energy Levels for an Elliptical Quantum Well with Zeeman Effect and SO Coupling	23
D	Fock-Darwin States for a Circular Quantum Well with Creation and Annihilation Operators	25

1 Introduction

Quantum dots are interesting systems both with respect to fundamental research as well as from a technological point of view, recently, in particular, for quantum computation. A quantum dot is a nanoscale system containing only a few electrons whose movements are confined in all three spatial directions. A quantum dot exhibits very strong quantum mechanical behaviour, while it is possible to control its size and the number of electrons it contains, making it excellent for measurements of quantum mechanical properties. The work presented here is relevant as a model of an anisotropic quantum dot.

First, the behaviour of an electron on a two-dimensional surface with a uniform magnetic field applied perpendicular to the plane of the electron will be examined. Subsequently, a confinement potential in the form of a parabolic quantum well is imposed also on the electron moving in the magnetic field. We will treat both the special case of a circular confinement potential as well as that of an elliptical one. Finally, the electron spin will be taken into consideration. Specifically, we will consider the effect on the energy levels of adding a Zeeman term and Rashba spin-orbit coupling.

2 Free Electron in a Uniform Magnetic Field

Here we consider a free electron of mass m , which can move in two directions x, y . A uniform magnetic field of magnitude B is applied in a direction orthogonal to the plane in which the electron moves. The Hamiltonian of this system is

$$\mathcal{H}_0 = \frac{1}{2m}(\Pi_x^2 + \Pi_y^2), \quad (1)$$

$$\vec{\Pi} = -i\hbar\nabla - e\vec{A}, \quad (2)$$

where $\vec{\Pi}$ is the canonical momentum and \vec{A} is the vector potential related to the magnetic field by $B\hat{k} = \nabla \times \vec{A}$. In order to transform the Hamiltonian into a familiar form we introduce a new set of coordinates,

$$\zeta = \Pi_y \qquad \eta = \frac{\Pi_x}{m\omega_c}$$

where $\omega_c = \frac{eB}{m}$ is the Larmor frequency. These variables are canonical, $[\eta, \zeta] = i\hbar$, which can be seen by choosing a gauge and evaluating the commutator. Substituting the new variables in the Hamiltonian it takes the form

$$\mathcal{H}_0 = \frac{1}{2m}\zeta^2 + \frac{1}{2}m\omega_c^2\eta^2. \quad (3)$$

In these variables it is simple to observe that the system is a harmonic oscillator at the Larmor frequency. The eigenenergies of the Hamiltonian are thus

$$E_N = (N + \frac{1}{2})\hbar\omega_c, \quad N = 0, 1, 2, \dots \quad (4)$$

With the purpose of identifying the wave functions in the (x, y) basis, we write the Hamiltonian in the original variables and choose the Landau gauge, $\vec{A} = Bx\hat{j}$ for the

vector potential. Then the Hamiltonian is

$$\mathcal{H}_0 = \frac{1}{2m} [p_x^2 + (p_y - eBx)^2]. \quad (5)$$

Using an eigenfunction of the form $\phi(x, y) = e^{ik_y y} \chi(x)$ the following one-dimensional equation can be obtained,

$$\frac{-\hbar^2}{2m} \frac{\partial^2 \chi(x)}{\partial x^2} + \frac{1}{2} m \omega_c^2 (x - X)^2 \chi(x) = E \chi(x), \quad (6)$$

where the displacement $X = k_y l_0^2$ and $l_0 = \sqrt{\frac{\hbar}{eB}}$ is the magnetic length.

In this form, it is evident that the Schrödinger equation describes a single harmonic oscillator oscillating at the Larmor frequency around the equilibrium point at X. The eigenfunctions are

$$\phi_{NX} = A_N e^{ik_y y} e^{-\frac{(x-X)^2}{2l_0^2}} H_N \left[\frac{(x-X)}{l_0} \right], \quad (7)$$

with

$$A_N = \left(\frac{m\omega_c}{\pi \hbar 2^{2N} (N!)^2} \right)^{1/4},$$

and H_N are Hermite polynomials.

The levels of this oscillator, called the Landau levels, are infinitely degenerate when the surface on which the electron moves is an infinite plane. This is because the system contains a high degree of symmetry; it is both translationally and rotationally invariant. When the system is confined to a rectangular cell with sides of lengths L_x and L_y , the degeneracy of each Landau level can be estimated as the number of allowed values of k_y such that the centre X lies between 0 and L_x . Using periodic boundary conditions in the y direction, $\phi(x, 0) = \phi(x, L_y)$ we obtain an expression for all k_y . Substituting the expression in $X = k_y l_0^2$ we find

$$X = \frac{2\pi N}{L_y} l_0^2. \quad (8)$$

The maximum number of allowed states, N_s for which $0 < X < L_x$ is then

$$N_s = \frac{L_x L_y}{2\pi l_0^2}. \quad (9)$$

The maximum number of allowed states can also be expressed as a function of the magnetic flux through the rectangular surface, $\Phi = L_x L_y B$,

$$N_s = \frac{\Phi}{2\pi B l_0^2} = \frac{\Phi}{\Phi_0}, \quad (10)$$

where $\Phi_0 = 2\pi\hbar/e$ is the flux quantum. Hence the degeneracy of each Landau level is just the magnetic flux through the rectangular cell in units of the flux quantum.

3 Fock-Darwin States for a Circular Quantum Well

In the previous section a boundary was artificially imposed on a free electron moving in an orthogonal uniform magnetic field. In this section we build the boundary into the theory by adding an isotropic parabolic confinement potential to the Hamiltonian of the previous section. This system was first studied by V. Fock [4] and C. G. Darwin [3].

Choosing the symmetrical gauge $\vec{A} = -\frac{1}{2}By\hat{i} + \frac{1}{2}Bx\hat{j}$, the Hamiltonian of a free electron in a uniform magnetic field, \mathcal{H}_0 can be put into the form,

$$\mathcal{H}_0 = \frac{1}{2m} (p_x^2 + p_y^2) + \frac{1}{2}m\omega_1^2 (x^2 + y^2) - \omega_1 (xp_y - yp_x), \quad (11)$$

where $\omega_1 = \omega_c/2$ is a rescaled Larmor frequency. We now add a quadratic confinement potential, $V_{conf} = \frac{1}{2}m\omega_0^2 (x^2 + y^2)$ to the Hamiltonian,

$$\begin{aligned} \mathcal{H} &= \mathcal{H}_0 + V_{conf} \\ &= \frac{1}{2m} (p_x^2 + p_y^2) + \frac{1}{2}m [\omega_1^2 + \omega_0^2] (x^2 + y^2) - \omega_1 (xp_y - yp_x). \end{aligned} \quad (12)$$

The corresponding Schrödinger equation is

$$\frac{\hbar^2}{2m} \nabla^2 \psi + E\psi - \frac{1}{2}m [\omega_1^2 + \omega_0^2] (x^2 + y^2) \psi - i\omega_1 \hbar \left(x \frac{\partial \psi}{\partial y} - y \frac{\partial \psi}{\partial x} \right) = 0. \quad (13)$$

Using the substitutions

$$\begin{aligned} b &= \left(\frac{\hbar}{m} \right)^{1/2} (\omega_1^2 + \omega_0^2)^{-1/4}, \\ w &= \frac{\omega_1}{\sqrt{\omega_1^2 + \omega_0^2}}, \\ W &= \frac{E}{\hbar \sqrt{\omega_1^2 + \omega_0^2}}, \end{aligned} \quad (14)$$

and switching to polar coordinates,

$$x = \xi b \cos \phi \quad y = \xi b \sin \phi \quad \xi = r/b \quad (15)$$

we obtain the following equation for ψ ,

$$\left[\frac{\partial^2 \psi}{\partial \xi^2} + \frac{1}{\xi} \frac{\partial \psi}{\partial \xi} + \frac{1}{\xi^2} \frac{\partial^2 \psi}{\partial \phi^2} \right] - 2iw \frac{\partial \psi}{\partial \phi} + (2W - \xi^2) \psi = 0. \quad (16)$$

Assuming that the angular part of the wave function can be written as a standing wave, $\psi = e^{in\phi} R(\xi)$, $n \in \mathbb{Z}$ we obtain a one-dimensional equation for the radial part, $R(\xi)$,

$$\frac{\partial^2 R}{\partial \xi^2} + \frac{1}{\xi} \frac{\partial R}{\partial \xi} + \left(2W_1 - \xi^2 - \frac{n^2}{\xi^2} \right) R = 0, \quad (17)$$

where the substitution $W_1 = W + nw$ has been made. Switching variable again to

$$\xi^2 = \rho, \quad (18)$$

we obtain the equation

$$\frac{\partial^2 R}{\partial \rho^2} + \frac{1}{\rho} \frac{\partial R}{\partial \rho} + \left(\frac{W_1}{2\rho} - \frac{n^2}{4\rho^2} - \frac{1}{4} \right) R = 0. \quad (19)$$

Since this equation is similar to that of the hydrogen atom, we look for solutions of the form $R(\rho) = \rho^{|n|/2} e^{-\rho/2} \lambda(\rho)$ and obtain the following equation for $\lambda(\rho)$,

$$\rho \frac{\partial^2 \lambda}{\partial \rho^2} + (|n| + 1 - \rho) \frac{\partial \lambda}{\partial \rho} + \frac{1}{2} (W_1 - |n| - 1) \lambda = 0. \quad (20)$$

This equation has solutions if and only if

$$W_1 = 2k + |n| + 1, \quad n \in \mathbb{Z}, \quad k = 0, 1, \dots \quad (21)$$

The eigenvalues can then be identified in terms of the energy,

$$E_{nk} = \hbar \omega_1 [(2k + |n| + 1) / w + n]. \quad (22)$$

A few low lying energy levels are plotted as a function of the confinement potential strength in Figure 1. The system under consideration is invariant with respect to

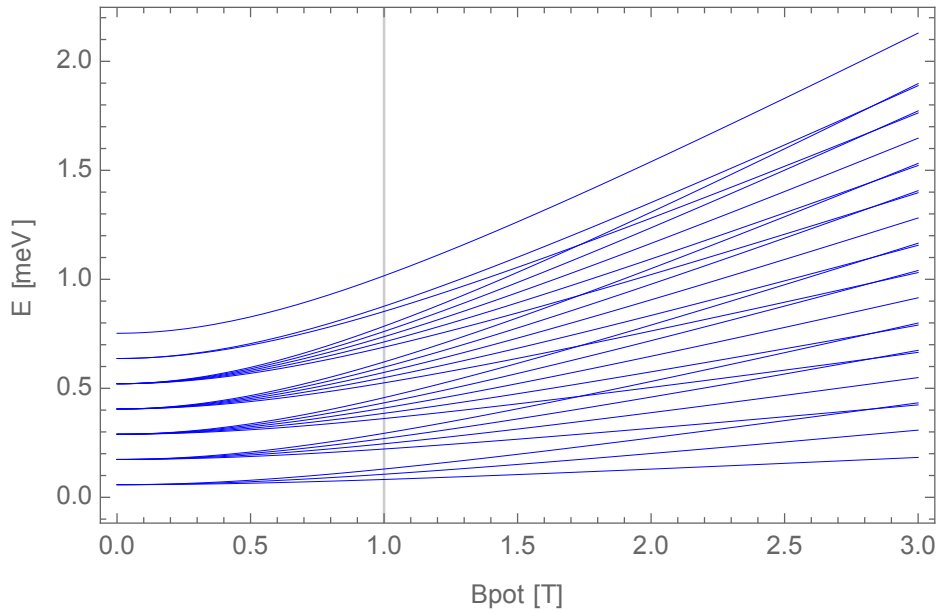


Figure 1: Plot of the energy levels with $n=-2, \dots, 2$, $k=0, \dots, 4$, as a function of the strength of the confinement potential. Energy is in units of meV, while the confinement potential strength is in units of T such that $\omega_0 = eB_{pot}/(2m)$. The vertical line at $B_{pot} = 1$ marks the value of the magnetic field strength, B .

rotations around the z axis. However, this invariance does not cause degeneracies in the spectrum. It is evident from the expression in eq. (22) that the energy levels are non-degenerate for arbitrary values of w , which can be between zero and one (depending on the ratio between the confinement potential strength and the magnetic field strength, ω_0/ω_1). Only when w takes on the limiting values does the spectrum simplify and degeneracies occur (with the exception of points of accidental degeneracies where the energy levels cross). This effect is evident from the figure, where the energy

levels very noticeably split as the confinement potential strength becomes significant compared to the magnetic field strength, and recombine in different combinations when the magnetic field becomes negligible. The plot implies that the energy levels take the form of equidistant harmonic oscillator energies in the limits where the confinement potential is either very weak or very strong compared to the magnetic field strength. By analyzing the expression for the energy levels, eq. (22) this behaviour can be verified. For large ω_0/ω_1 where $w \rightarrow 0$,

$$\begin{aligned} E_{s_1 s_2} &\sim \hbar\omega_0(2k + |n| + 1) \\ &\equiv \hbar\omega_0(s_1 + s_2 + 1), \quad s_1, s_2 = 0, 1, \dots \end{aligned}$$

where $s_{1,2} = k + (|n| \pm n)/2$. These are the energy levels of a two-dimensional harmonic oscillator with a frequency of ω_0 . In this limit, the energy levels contain degeneracies because the system becomes invariant under time reversal as the effect of the magnetic field becomes negligible. Mathematically, the degeneracies are exclusively due to the multiplicity of values for s_1 and s_2 that will add up to a given number, such that the degeneracy of $E_{s_1 s_2}$ is $s_1 + s_2 + 1$. This is because the multiplicity of choices for k and n that combine to give a specific set of (s_1, s_2) turns out to be one at every level. In Figure 2 this degeneracy is easily recognizable.

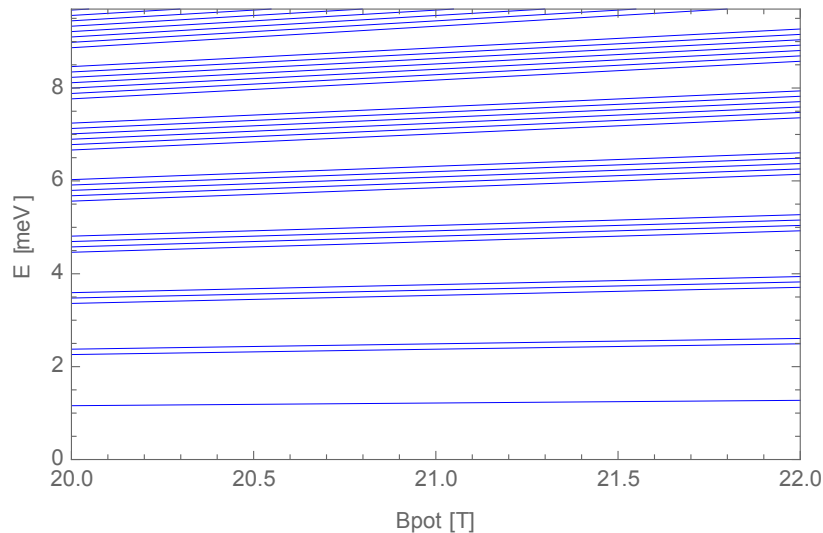


Figure 2: Plot of the low lying energy levels in the large ω_0/ω_1 limit. The quantum numbers take values $n=-8, \dots, 8$, $k=0, \dots, 7$ (however, not every level corresponding to these quantum numbers is included in the plot). The value of the magnetic field strength is $B = 1$ T. Energy is in units of meV, while the confinement potential strength is in units of T such that $\omega_0 = eB_{pot}/(2m)$.

For small ω_0/ω_1 where $w \rightarrow 1$,

$$E_s \sim \hbar\omega_c \left(s + \frac{1}{2} \right), \quad s = 0, 1, \dots$$

Translational symmetry is restored to the system and the energy levels of the Fock-Darwin states reduce to those of a free electron in a magnetic field with $s = k + (|n| + n)/2$. Those are the infinitely degenerate Landau levels found in the previous section, where the infinite degeneracy comes from the fact that any $n \leq 0$ will make

the second term in s zero (in Figure 1 the degeneracy appears to be finite because only three non-positive n 's are included).

To identify the eigenfunctions we substitute the eigenenergies, E_{nk} in eq. (20) and obtain the equation

$$\rho \frac{\partial^2 \lambda}{\partial \rho^2} + (|n| + 1 - \rho) \frac{\partial \lambda}{\partial \rho} + k\lambda = 0. \quad (23)$$

This is Laguerre's associated differential equation. Its solutions are the associated Laguerre polynomials $\lambda(\rho) = L_{|n|+k}^{|n|}(\rho)$. Then the solution to the radial equation is

$$R(\rho) = \rho^{|n|/2} e^{-\rho/2} L_{|n|+k}^{|n|}(\rho). \quad (24)$$

The normalized wave functions, ψ_{nk} are

$$\psi_{nk}(r, \phi) = N e^{in\phi} \left(\frac{r}{b}\right)^{|n|} e^{-(r/b)^2/2} L_{|n|+k}^{|n|} \left[\left(\frac{r}{b}\right)^2 \right], \quad (25)$$

with

$$N = (|n| + k)! [\pi b^2 (3|n| + 2k)! {}_2F_1(-|n| - k, -2|n| - k; -3|n| - 2k; 1)]^{-1/2},$$

where we have transformed back to polar coordinates. ${}_2F_1$ is Gauss' Hypergeometric Function. The norm squared of the wave function of a specific state is illustrated in Figure 3.

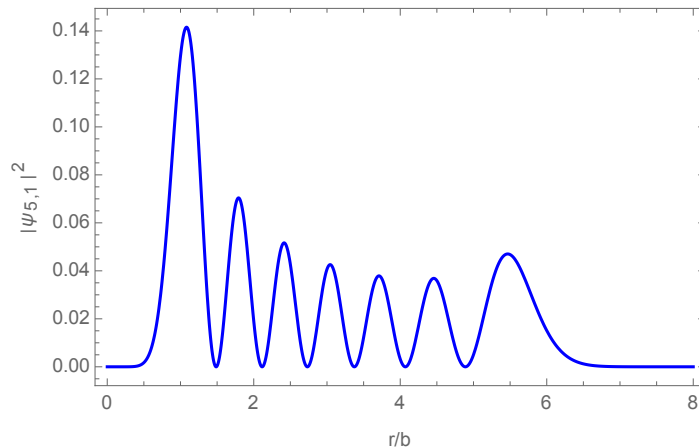


Figure 3: Plot of the norm squared of the wave function with $n = 5$, $k = 1$, $|\psi_{5,1}(r)|^2$ as a function of r in units of b .

Evidently, the probability density of any state is independent of ϕ but varies with r and will therefore form circular rings of high probability around the centre of the confinement potential.

3.1 Properties of Fock-Darwin States for a Circular Quantum Well

To gain some insight as to the behaviour of the Fock-Darwin states we will investigate the probability current density and the magnetic moment of these states.

The probability current density of the system is

$$\vec{J} = \frac{\hbar}{2mi} (\psi^* \nabla \psi - \psi \nabla \psi^*).$$

Working in polar coordinates, it can be shown that

$$\begin{aligned} \psi^* \nabla \psi = & \frac{in|N|^2}{b} \rho^{|n|-1/2} e^{-\rho} \left(L_{|n|+k}^{|n|} \right)^2 \hat{e}_\phi + \\ & \frac{|N|^2}{b} \rho^{|n|-1/2} e^{-\rho} \left[-2\rho L_{|n|+k}^{|n|} L_{|n|+k-1}^{|n|+1} + |n| \left(L_{|n|+k}^{|n|} \right)^2 - \rho \left(L_{|n|+k}^{|n|} \right)^2 \right] \hat{e}_r, \end{aligned}$$

where the variable $\rho = \xi^2$ has been suppressed in the associated Laguerre polynomials. Since the radial component in the above is real,

$$J_r = 0, \quad (26)$$

which means that no current can flow in the radial direction, since none of the states produces such a current. The angular component of the probability current density is

$$J_\phi = \frac{|N|^2 \hbar}{mb} n \rho^{|n|-1/2} e^{-\rho} \left[L_{|n|+k}^{|n|}(\rho) \right]^2. \quad (27)$$

The angular component of the probability current densities of three specific states are illustrated in Figure 4. In Figure 5 the probability current densities of the same three states are illustrated as vector fields.

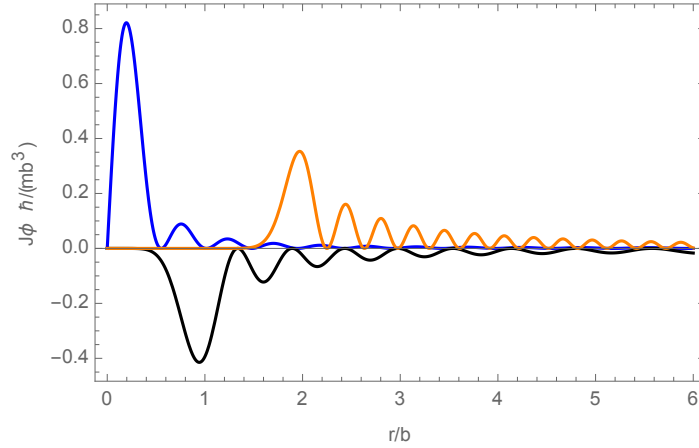


Figure 4: Plot of the angular component of the probability current density, $J_\phi(r)$ with $(n, k) = (1, 10)$ (blue), $(-5, 3)$ (black), $(22, 5)$ (orange) in units of $\hbar/(mb^3)$, as a function of r in units of b . The maximum electric current through a line of length b for each state is 17 nA (blue), 8.7 nA (black), 7.4 nA (orange).

Since J_ϕ is independent of ϕ but varies in the radial direction, the probability current density of any one state will form rings around the centre of the confinement potential. Notice that the quantum number n determines the direction of the current flow. For $n = 0$ the probability current is zero everywhere, while for $n < 0$ the probability current runs clockwise and for $n > 0$ it runs counter-clockwise. Apart from this, the role of the quantum number n is to change the ratio of the height of the first peak in J_ϕ to the height of the other peaks (the first peak is always tallest) as well as to

change the radius at which the first peak is centred. For small $|n|$ the first peak is very tall compared to the other peaks and it is situated at a small radius from the centre of the confinement potential. For large $|n|$ the opposite is true of the ratio of the heights and the radius at which the peak is centred.

The quantum number k changes the heights of all the peaks simultaneously while not affecting the ratios of the peak heights. For small k one obtains low and rather wide peaks and for large k the peaks are narrow and tall. The number of peaks in J_ϕ is $|n| + k + 1$ except when $n = 0$.

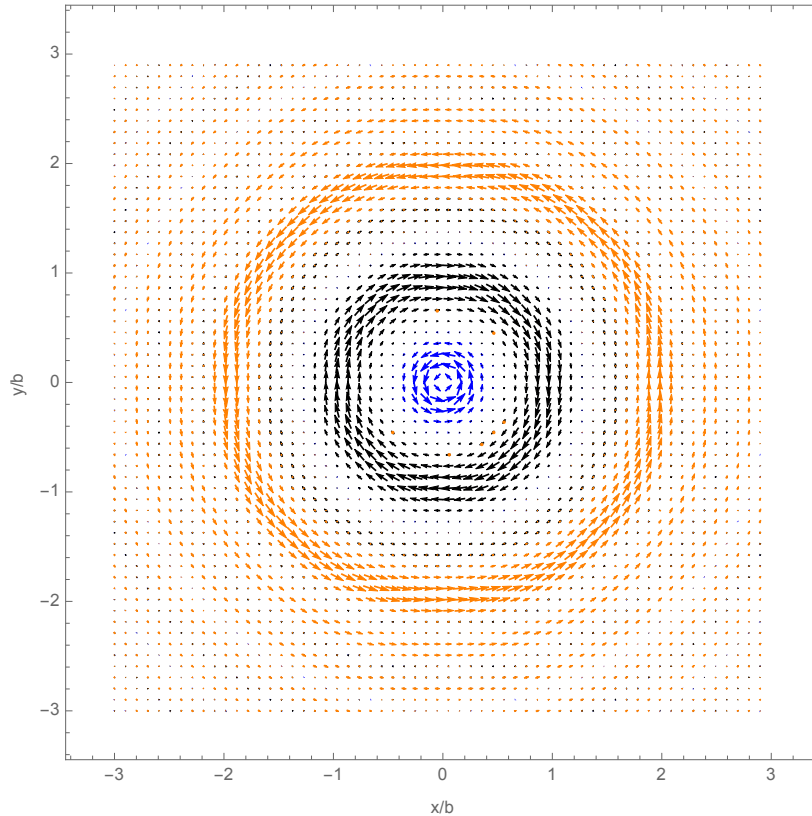


Figure 5: Plot of the probability current density vector field, \vec{J} in the $x/b, y/b$ plane. The same quantum numbers are used as in Figure 4, namely $(n, k) = (1, 10)$ (blue), $(-5, 3)$ (black), $(22, 5)$ (orange).

Associated with each state n, k there is a magnetic moment, M_{nk} , which can be found by differentiating the energy with respect to the magnetic field strength, B ,

$$M_{nk} = -\frac{\partial E_{nk}}{\partial B} = -\mu_B [(2k + |n| + 1)w + n], \quad (28)$$

where $\mu_B = e\hbar/(2m)$ is the Bohr magneton. The average value of the total magnetic moment, $\langle M \rangle$ can be found from the partition function,

$$\langle M \rangle = \frac{1}{\beta} \frac{\partial \log Z}{\partial B}$$

where

$$Z = \prod_{n,k} (e^{(\mu - E_{nk})\beta} + 1). \quad (29)$$

In the above μ is the chemical potential and $\beta = 1/T$, where T is the temperature. By manipulating the above expressions the average total magnetic moment can be written as

$$\begin{aligned} \langle M \rangle &= \sum_{n,k} (e^{(E_{nk}-\mu)\beta} + 1)^{-1} M_{nk} \\ &= - \sum_{n,k} f(E_{nk}, \mu) \mu_B [(2k + |n| + 1)\omega + n], \end{aligned} \quad (30)$$

where $f(E_{nk}, \mu)$ is the Fermi-Dirac distribution function. It is interesting also to find the magnetic moment through a semi-classical analysis to gain some intuition and to illustrate the equivalence of the quantum mechanical analysis and the semi-classical one in the high energy limit. We use $\vec{j} = -e\vec{J}$ for the current density and the classical definition,

$$\overrightarrow{dM} = \frac{1}{2} \vec{r} \times \vec{j}$$

for the differential magnetic moment. The magnetic moment, M can then be found from dM by integrating over all of space.

$$\begin{aligned} M &= \int_{all\ space} dM\ dA \\ &= -\mu_B n \pi |N|^2 \int_0^\infty \rho^{|n|} e^{-\rho} \left[L_{|n|+k}^{(|n|)}(\rho) \right]^2 d\rho \\ &= -\mu_B n. \end{aligned} \quad (31)$$

This corresponds to the behaviour of eq. (28) in the high energy limit ($\omega \rightarrow 0$) for which $M_{nk} \rightarrow -\mu_B n$. Since the current is in the ϕ direction, classically the magnetic moment will be directed along the positive z axis.

4 Fock-Darwin States for an Elliptical Quantum Well

We now interest ourselves in deriving an analytical solution for the Fock-Darwin states and energy levels for an anisotropic well, i.e. for an elliptical confinement potential. This potential takes the specific form;

$$V_{conf} = \frac{1}{2} m (\omega_x^2 x^2 + \omega_y^2 y^2). \quad (32)$$

Again we choose the symmetrical gauge, $\vec{A} = -\frac{1}{2} B y \hat{i} + \frac{1}{2} B x \hat{j}$, so the Hamiltonian can be written as

$$\mathcal{H} = \frac{1}{2m} [p_x^2 + p_y^2 + m^2 (\omega_1^2 + \omega_x^2) x^2 + m^2 (\omega_1^2 + \omega_y^2) y^2 + 2m\omega_1 (p_x y - p_y x)]. \quad (33)$$

Defining the effective frequencies (scaled by the mass, m) in the x, y directions respectively,

$$\Omega_{1,2}^2 = m^2 (\omega_1^2 + \omega_{x,y}^2) \quad (34)$$

the Hamiltonian is

$$\mathcal{H} = \frac{1}{2m} [p_x^2 + p_y^2 + \Omega_1^2 x^2 + \Omega_2^2 y^2 + 2m\omega_1 (p_x y - p_y x)]. \quad (35)$$

We are interested in discovering a canonical transformation of variables such that the Hamiltonian is diagonal in the new generalized coordinates. We choose a transformation of the form

$$\begin{aligned} q_1 &= \cos \chi x + \chi_2 \sin \chi p_y & p_2 &= -\chi_1 \sin \chi x + \cos \chi p_y \\ q_2 &= \cos \chi y + \chi_2 \sin \chi p_x & p_1 &= -\chi_1 \sin \chi y + \cos \chi p_x, \end{aligned} \quad (36)$$

where $\chi, \chi_1, \chi_2 \in \mathbb{R}$ are free parameters. The above transformation is canonical if

$$\chi_1 \chi_2 = 1. \quad (37)$$

The details of how we arrive at the above form for a canonical transformation are included in Appendix A. In the new coordinates defined in eqs. (36) the Hamiltonian becomes

$$\begin{aligned} \mathcal{H} &= \frac{p_1^2}{4m} (1 + \chi_2^2 \Omega_2^2 + \cos 2\chi - \chi_2^2 \Omega_2^2 \cos 2\chi - 2m\omega_1 \chi_2 \sin 2\chi) + \\ &\frac{p_2^2}{4m} (1 + \chi_2^2 \Omega_1^2 + \cos 2\chi - \chi_2^2 \Omega_1^2 \cos 2\chi + 2m\omega_1 \chi_2 \sin 2\chi) + \\ &\frac{q_1^2}{4m} (\chi_1^2 + \Omega_1^2 - \chi_1^2 \cos 2\chi + \Omega_1^2 \cos 2\chi - 2m\omega_1 \chi_1 \sin 2\chi) + \\ &\frac{q_2^2}{4m} (\chi_1^2 + \Omega_2^2 - \chi_1^2 \cos 2\chi + \Omega_1^2 \cos 2\chi + 2m\omega_1 \chi_1 \sin 2\chi) + \\ &\frac{q_1 p_2}{2m} (-2m\omega_1 \cos 2\chi + \chi_1 \sin 2\chi - \chi_2 \Omega_1^2 \sin 2\chi) + \\ &\frac{q_2 p_1}{2m} (2m\omega_1 \cos 2\chi + \chi_1 \sin 2\chi - \chi_2 \Omega_2^2 \sin 2\chi). \end{aligned} \quad (38)$$

By demanding that the coefficients of the off-diagonal terms in the Hamiltonian be equal to zero we obtain

$$\chi_1^2 = \frac{\Omega_1^2 + \Omega_2^2}{2}, \quad (39)$$

$$\tan 2\chi = 2m\omega_1 [2(\Omega_1^2 + \Omega_2^2)]^{1/2} / (\Omega_1^2 - \Omega_2^2). \quad (40)$$

Defining

$$\Omega_3^2 = [(\Omega_1^2 - \Omega_2^2)^2 + 8m^2\omega_1^2 (\Omega_1^2 + \Omega_2^2)]^{1/2} \quad (41)$$

the Hamiltonian is

$$\mathcal{H} = \frac{1}{2m} (\alpha_1^2 p_1^2 + \alpha_2^2 p_2^2 + \beta_1^2 q_1^2 + \beta_2^2 q_2^2) \quad (42)$$

with

$$\begin{aligned} \alpha_1^2 &= \frac{\Omega_1^2 + 3\Omega_2^2 + \Omega_3^2}{2(\Omega_1^2 + \Omega_2^2)} & \alpha_2^2 &= \frac{3\Omega_1^2 + \Omega_2^2 - \Omega_3^2}{2(\Omega_1^2 + \Omega_2^2)} \\ \beta_1^2 &= \frac{1}{4} (3\Omega_1^2 + \Omega_2^2 + \Omega_3^2) & \beta_2^2 &= \frac{1}{4} (\Omega_1^2 + 3\Omega_2^2 - \Omega_3^2). \end{aligned} \quad (43)$$

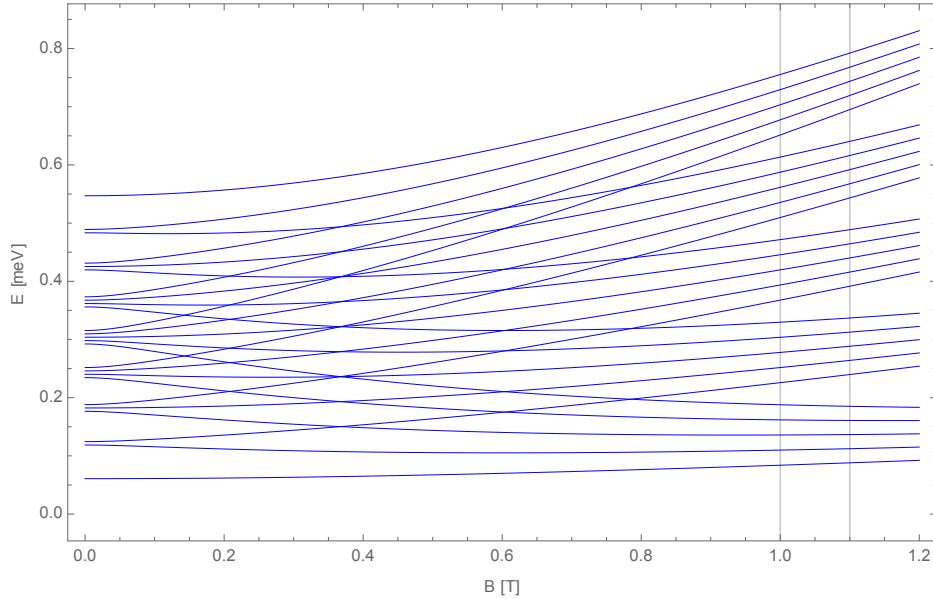


Figure 6: Plot of the energy levels of the anisotropic Fock-Darwin states with $n_1, n_2 = 0, \dots, 4$, as a function of the magnetic field strength. The vertical lines at $B = 1$ T, 1.1 T mark the values of the confinement potential strengths in the x, y directions such that $\omega_{x,y} = eB_{potx,y}/(2m)$.

The eigenenergies are those of two harmonic oscillators in the q_1, q_2 directions,

$$E_{n_1 n_2} = \left(n_1 + \frac{1}{2}\right) \hbar\omega'_1 + \left(n_2 + \frac{1}{2}\right) \hbar\omega'_2, \quad n_1, n_2 = 0, 1, \dots \quad (44)$$

with $\omega'_{1,2} = \alpha_{1,2}\beta_{1,2}/m$. A few low lying energy levels are plotted in Figure 6.

The elliptical Fock-Darwin Hamiltonian is invariant with respect to mirroring in the x and y axes respectively, but these discrete symmetries do not cause degeneracies in the spectrum for arbitrary values of $\omega'_{1,2}$ (equivalently $\omega_{x,y}/\omega_1$). When the magnetic field is zero the system behaves as two harmonic oscillators in the x, y directions ($\omega'_1 = \omega_x$ and $\omega'_2 = \omega_y$). In this limit, the system becomes invariant under time reversal, however, degeneracies do not appear as in the case of a circular confinement potential, because the two-dimensional harmonic oscillator obtained in this limit is still anisotropic.

When the magnetic field strength is very large the system behaves as one harmonic oscillator at the Larmor frequency ($\omega'_1 = \omega_c$ and $\omega'_2 = 0$) with infinitely degenerate Landau levels, just as the isotropic system did in the same limit (the degeneracy of the energy levels in Figure 6 appears to be finite because of the finite range of quantum numbers that are included). Mathematically, the infinite degeneracy in this case stems from the fact that changing the value of n_2 leaves the energy unchanged.

When the elliptical confinement potential is stretched substantially in one direction and compressed in the other, $\omega_y/\omega_x \ll 1$, the energy levels reduce to those of one harmonic oscillator at an effective frequency $\omega'_1 = \sqrt{\omega_c^2 + \omega_x^2}$ ($\omega'_2 = 0$), again with infinitely degenerate energy levels. Notice that for $\omega_x = \omega_y \equiv \omega_0$ the energy levels of the anisotropic Fock-Darwin states reduce appropriately to

$$E_{n_1 n_2} = \hbar\omega_1 [(n_1 + n_2 + 1)/w + (n_1 - n_2)], \quad (45)$$

which is equivalent to eq. (22) for $n_{1,2} = k + (|n| \pm n)/2$.

Since the transformed Hamiltonian is a two-dimensional harmonic oscillator, we can construct creation and annihilation operators in (q, p) space that will facilitate further calculations. Define

$$\begin{aligned} a_1 &= \frac{\beta_1}{(2m\hbar\omega'_1)^{1/2}}q_1 + i\frac{\alpha_1}{(2m\hbar\omega'_1)^{1/2}}p_1, \\ a_1^\dagger &= \frac{\beta_1}{(2m\hbar\omega'_1)^{1/2}}q_1 - i\frac{\alpha_1}{(2m\hbar\omega'_1)^{1/2}}p_1, \\ a_2 &= \frac{\beta_2}{(2m\hbar\omega'_2)^{1/2}}q_2 + i\frac{\alpha_2}{(2m\hbar\omega'_2)^{1/2}}p_2, \\ a_2^\dagger &= \frac{\beta_2}{(2m\hbar\omega'_2)^{1/2}}q_2 - i\frac{\alpha_2}{(2m\hbar\omega'_2)^{1/2}}p_2. \end{aligned} \quad (46)$$

Then the Hamiltonian in eq. (42) can be written

$$\mathcal{H} = (a_1^\dagger a_1 + \frac{1}{2})\hbar\omega'_1 + (a_2^\dagger a_2 + \frac{1}{2})\hbar\omega'_2. \quad (47)$$

To identify the ground state, $\langle x, y|0\rangle = \psi_{00}(x, y)$ we exploit that it must be annihilated by both a_1 and a_2 .

$$\begin{aligned} a_1 |0\rangle &= 0, \\ a_2 |0\rangle &= 0. \end{aligned} \quad (48)$$

In the position basis expressed in (x, y) coordinates eqs. (48) take the form,

$$\begin{aligned} \left[\beta_1 \cos \chi x + \alpha_1 \hbar \cos \chi \frac{\partial}{\partial x} - i\alpha_1 \chi_1 \sin \chi y - i\beta_1 \chi_2 \hbar \sin \chi \frac{\partial}{\partial y} \right] \psi_{00} &= 0, \\ \left[-i\alpha_2 \chi_1 \sin \chi x - i\beta_2 \chi_2 \hbar \sin \chi \frac{\partial}{\partial x} + \beta_2 \cos \chi y + \alpha_2 \hbar \cos \chi \frac{\partial}{\partial y} \right] \psi_{00} &= 0. \end{aligned} \quad (49)$$

We use the ansatz; $\psi_{00} = N_0 \exp \left[-\frac{1}{2\hbar} (ax^2 + by^2 + cxy) \right]$ where $a, b, c \in \mathbb{C}$ and obtain the equations

$$\begin{aligned} x(\beta_1 \cos \chi - \alpha_1 \cos \chi a + i\beta_1 \chi_2 \sin \chi c) + y(i\beta_1 \chi_2 \sin \chi b - i\alpha_1 \chi_1 \sin \chi - \alpha_1 \cos \chi c) &= 0, \\ x(i\beta_2 \chi_2 \sin \chi a - i\alpha_2 \chi_1 \sin \chi - \alpha_2 \cos \chi c) + y(\beta_2 \cos \chi - \alpha_2 \cos \chi b + i\beta_2 \chi_2 \sin \chi c) &= 0. \end{aligned} \quad (50)$$

By demanding that the coefficients of x and y be zero in the above equations we obtain a solution for a, b, c :

$$a = \alpha_2 \beta_1 / \gamma \quad b = \alpha_1 \beta_2 / \gamma \quad c = i\chi_2 \sin 2\chi (\beta_1 \beta_2 - \alpha_1 \alpha_2 \chi_1^2) / \gamma, \quad (51)$$

where

$$\gamma = \cos^2 \chi \alpha_1 \alpha_2 + \sin^2 \chi \beta_1 \beta_2 \chi_2^2. \quad (52)$$

Hence, the ground state wave functions is

$$\psi_{00} = N_0 \exp \left[-\frac{1}{2\hbar\gamma} (\alpha_2 \beta_1 x^2 + \alpha_1 \beta_2 y^2 + i\chi_2 \sin 2\chi (\beta_1 \beta_2 - \alpha_1 \alpha_2 \chi_1^2) xy) \right], \quad (53)$$

with

$$N_0 = \left(\frac{\alpha_1 \alpha_2 \beta_1 \beta_2}{\pi^2 \hbar^2 \gamma^2} \right)^{1/4}.$$

Evidently, the norm squared of the ground state is an anisotropic Gaussian in two dimensions. The excited states can be found by application of the creation operators from eqs. (46),

$$|n_1 n_2\rangle = \frac{(a_1^\dagger)^{n_1} (a_2^\dagger)^{n_2}}{(n_1!)^{1/2} (n_2!)^{1/2}} |0\rangle. \quad (54)$$

Figure 7 shows plots of the norm squared of the first nine wave functions.

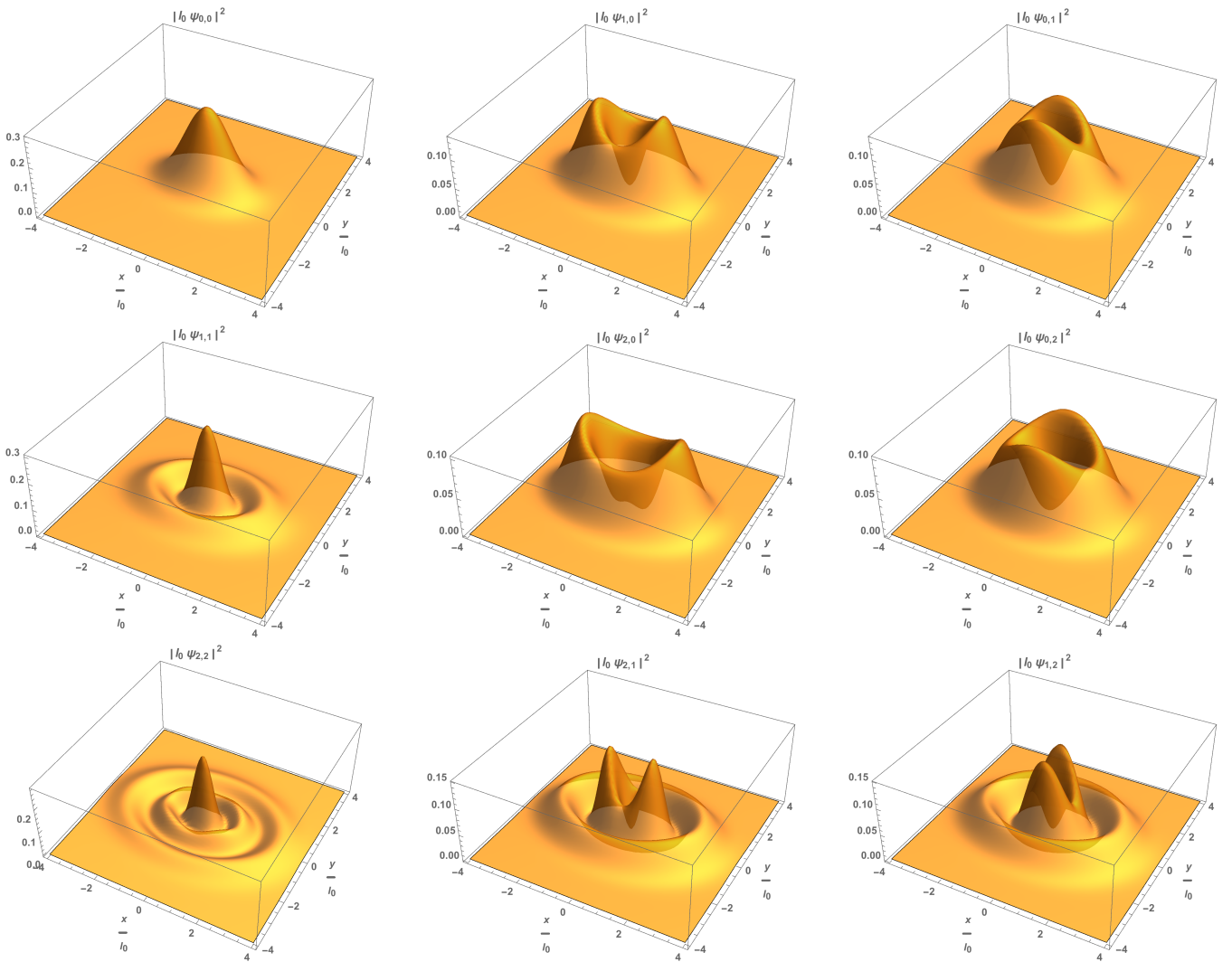


Figure 7: The norm squared of the wave functions of the first nine anisotropic Fock-Darwin states, $n_1, n_2 = 0, 1, 2$. The quantum numbers are specified in the label above each plot. Distance is measured in units of the magnetic length l_0 while the wave functions have been multiplied by l_0 . The magnetic field strength is $B = 1$ T and the confinement potential parameters are $B_{potx} = 1$ T, $B_{poty} = 2$ T, where $\omega_{x,y} = eB_{potx,y}/(2m)$.

Notice that for all the states displayed in Figure 7, the regions of high probability density form elliptical rings around the centre of the confinement potential. However, the magnitude of the probability density on the elliptical rings does not necessarily remain constant. Particles in states with $n_1 > n_2$ have a greater probability of being found close to the x axis, whereas, particles in states with $n_1 < n_2$ are more likely to be found close to the y axis.

4.1 Properties of Fock-Darwin States for an Elliptical Quantum Well

The probability current density, \vec{J} of the first nine anisotropic Fock-Darwin states are illustrated in Figure 8 as vector fields.

The regions of non-zero probability current density are all elliptical in shape and concentric to the confinement potential. The area of non-zero current reaches further away from the centre when the quantum numbers are increased (equivalently, when the energy is increased).

When $n_1 \neq n_2$ the current flows in elliptical rings around the center. The plots in Figure 8 imply that the direction of the current of any specific state is determined by the quantum numbers. For $n_1 > n_2$ the probability current density flows clockwise, whereas, for $n_1 < n_2$ it flows counter-clockwise. This analysis is consistent in the limit where the elliptical potential becomes circular. The direction of the probability currents generated by the Fock-Darwin states for the circular confinement potential is decided by the sign of the quantum number $n \in \mathbb{Z}$. From eq. (45) it was deduced that the quantum numbers of the energy levels for the elliptical and circular quantum wells are related thus, $n_{1,2} = k + (|n| \pm n)/2$. From this expression it is evident, that $n_1 = n_2$ if and only if $n = 0$. Then the probability currents disappear for the circular case, while for the elliptical case they have no overall direction, rather, they tend to form whirls of current. When $n > 0$, then $n_1 = k + |n|$ and $n_2 = k$, hence $n_1 > n_2$ and the probability current flows clockwise for both the elliptical and circular potential. When $n < 0$, then $n_1 < n_2$ and the probability current flows counter-clockwise for both potentials.

The plots in Figure 8 also imply that the probability currents contain another feature determined by the quantum numbers, namely, where on the elliptical rings the current is strongest. When $n_1 > n_2$ the points on the elliptical rings where the current is greatest in magnitude are those close to the y axis. For $n_1 < n_2$ it is those close to the x axis.

The maximum electric current through one magnetic length, l_0 of one electron in each of the nine lowest states is

n_1, n_2	0,0	1,0	0,1	1,1	2,0	0,2	2,1	1,2	2,2
Max. current per l_0 [nA]	0.886	3.98	4.84	1.34	3.79	4.56	5.68	5.66	2.91

It is possible, but rather tedious, to derive an analytical expression for the magnetic moment of any single state, $M_{n_1 n_2}$ using the expression for the energy levels and $M_{n_1 n_2} = -\frac{\partial E_{n_1 n_2}}{\partial B}$. However, we have obtained numerical values for $M_{n_1 n_2}$ by way of this relation.

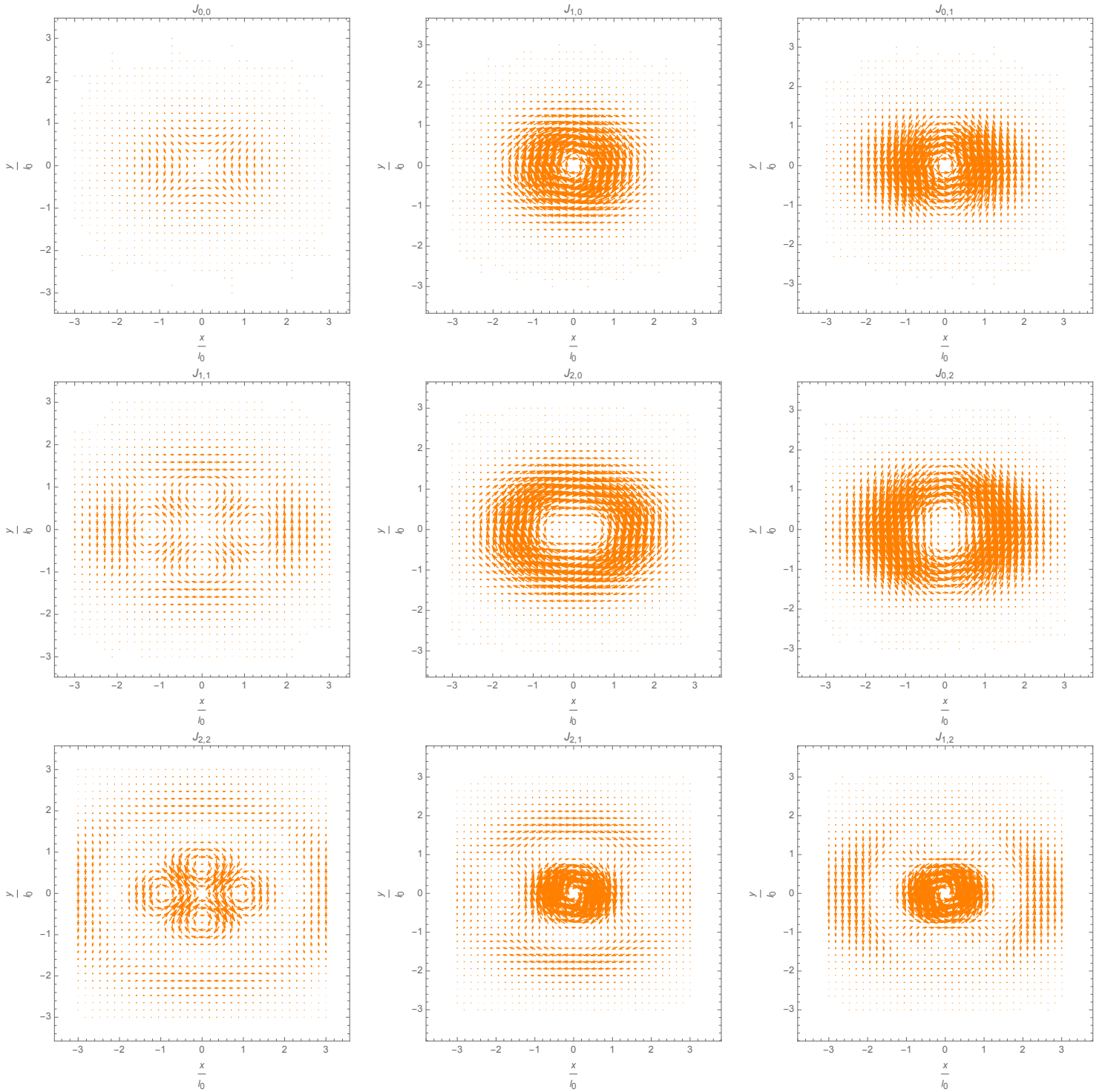


Figure 8: The probability current density, \vec{J} of the first nine anisotropic Fock-Darwin states, $n_1, n_2 = 0, 1, 2$. The quantum numbers are specified in the label above each plot. Distance is measured in units of the magnetic length l_0 . The magnetic field strength is $B = 1$ T and the confinement potential parameters are $B_{potx} = 1$ T, $B_{poty} = 2$ T, where $\omega_{x,y} = eB_{potx,y}/(2m)$.

5 Spin

We will now consider the spin of the electron in the elliptical Fock-Darwin potential. The spin effects regarded here are the Zeeman effect and the Rashba spin-orbit coupling. Including spin, the Hamiltonian will thus take the form

$$\mathcal{H} = \sum_{i=1,2} (a_i^\dagger a_i + \frac{1}{2}) \hbar \omega'_i + \mathcal{H}_Z + \mathcal{H}_{SO}, \quad (55)$$

$$\mathcal{H}_Z = -\vec{\mu} \cdot \vec{B}, \quad (56)$$

$$\mathcal{H}_{SO} = \frac{\lambda}{\hbar} \left[\vec{\sigma} \times (\vec{p} - e\vec{A}) \right]_z, \quad (57)$$

where μ is the spin magnetic moment, $\vec{\sigma} = \sigma_x \hat{i} + \sigma_y \hat{j} + \sigma_z \hat{k}$, and σ_i is the i 'th Pauli matrix. First we will treat the Zeeman effect and then the full Hamiltonian above.

5.1 Zeeman Effect

We now consider the Hamiltonian consisting of the anisotropic confinement potential and a Zeeman term:

$$\mathcal{H} = \sum_{i=1,2} (a_i^\dagger a_i + \frac{1}{2}) \hbar \omega'_i + \mathcal{H}_Z, \quad (58)$$

$$\mathcal{H}_Z = -\vec{\mu} \cdot \vec{B} = \hbar \omega_1 \sigma_z. \quad (59)$$

To incorporate the spin degree of freedom, we can construct the product basis $|n_1, n_2, s_z\rangle = |n_1, n_2\rangle |s_z\rangle$, where we have attached a spin quantum number, s_z which is the spin-component along the z direction, to the harmonic oscillator eigenstates of the previous section. In this basis the Zeeman effect will be simple to treat, as the Zeeman term is proportional to the z Pauli spin matrix. Hence $|n_1, n_2, s_z\rangle$ is an eigenstate of the Hamiltonian, eq. (58).

$$\begin{aligned} \mathcal{H} |n_1, n_2, s_z\rangle &= \left(\sum_{i=1,2} (a_i^\dagger a_i + \frac{1}{2}) \hbar \omega'_i + \hbar \omega_1 \sigma_z \right) |n_1, n_2, s_z\rangle \\ &= \left(\sum_{i=1,2} (n_i + \frac{1}{2}) \hbar \omega'_i + s_z \hbar \omega_1 \right) |n_1, n_2, s_z\rangle, \end{aligned} \quad (60)$$

where $s_z = \pm 1$. The effect of the Zeeman term is evidently to split the energy levels according to spin.

5.2 Rashba Spin-Orbit Coupling

We will now investigate the Rashba spin-orbit coupling term of the full Hamiltonian, eq. (55).

$$\mathcal{H} = \sum_{i=1,2} (a_i^\dagger a_i + \frac{1}{2}) \hbar \omega'_i + \mathcal{H}_Z + \mathcal{H}_{SO}, \quad (61)$$

$$\mathcal{H}_{SO} = \frac{\lambda}{\hbar} \left[\vec{\sigma} \times (\vec{p} - e\vec{A}) \right]_z, \quad (62)$$

Transforming to (q, p) space the spin-orbit term becomes

$$\begin{aligned} \frac{\hbar}{\lambda} \mathcal{H}_{SO} = & \sigma_x q_1 (\chi_1 \sin \chi - m\omega_1 \cos \chi) - \\ & \sigma_y q_2 (\chi_1 \sin \chi + m\omega_1 \cos \chi) - \\ & \sigma_y p_1 (\cos \chi - m\omega_1 \chi_2 \sin \chi) + \\ & \sigma_x p_2 (\cos \chi + m\omega_1 \chi_2 \sin \chi). \end{aligned} \quad (63)$$

We introduce the shorthand notation,

$$\begin{aligned} r_1 &= \left(\frac{m\hbar\omega'_1}{2\beta_1^2} \right)^{1/2} (\chi_1 \sin \chi + m\omega_1 \cos \chi), \\ r_2 &= \left(\frac{m\hbar\omega'_2}{2\beta_2^2} \right)^{1/2} (\chi_1 \sin \chi + m\omega_1 \cos \chi), \\ f_1 &= \left(\frac{m\hbar\omega'_1}{2\alpha_1^2} \right)^{1/2} (m\omega_1 \chi_2 \sin \chi - \cos \chi), \\ f_2 &= \left(\frac{m\hbar\omega'_2}{2\alpha_2^2} \right)^{1/2} (m\omega_1 \chi_2 \sin \chi + \cos \chi). \end{aligned} \quad (64)$$

In terms of the creation and annihilation operators in eqs. (46) the spin-orbit term is

$$\frac{\hbar}{\lambda} \mathcal{H}_{SO} = \sigma_x (a_1^\dagger + a_1) r_1 + \sigma_y (a_2^\dagger + a_2) r_2 + i\sigma_y (a_1^\dagger - a_1) f_1 + i\sigma_x (a_2^\dagger - a_2) f_2. \quad (65)$$

In the basis $|n_1, n_2, s_z\rangle$ the spin-orbit term is off-diagonal in the spin quantum number, since $\sigma_y |\uparrow\rangle = i|\downarrow\rangle$, $\sigma_y |\downarrow\rangle = -i|\uparrow\rangle$, $\sigma_x |\uparrow\rangle = |\downarrow\rangle$, $\sigma_x |\downarrow\rangle = |\uparrow\rangle$.

$$\langle n'_1, n'_2, \uparrow | \mathcal{H}_{SO} | n_1, n_2, \uparrow \rangle = 0, \quad (66)$$

$$\langle n'_1, n'_2, \downarrow | \mathcal{H}_{SO} | n_1, n_2, \downarrow \rangle = 0. \quad (67)$$

The remaining entries are

$$\begin{aligned} \langle n'_1, n'_2, \uparrow | \frac{\hbar}{\lambda} \mathcal{H}_{SO} | n_1, n_2, \downarrow \rangle = & r_1 \left[(n_1 + 1)^{1/2} \delta_{n'_1, n_1+1} + n_1^{1/2} \delta_{n'_1, n_1-1} \right] \delta_{n'_2, n_2} \\ & - ir_2 \left[(n_2 + 1)^{1/2} \delta_{n'_2, n_2+1} + n_2^{1/2} \delta_{n'_2, n_2-1} \right] \delta_{n'_1, n_1} \\ & + f_1 \left[(n_1 + 1)^{1/2} \delta_{n'_1, n_1+1} - n_1^{1/2} \delta_{n'_1, n_1-1} \right] \delta_{n'_2, n_2} \\ & + if_2 \left[(n_2 + 1)^{1/2} \delta_{n'_2, n_2+1} - n_2^{1/2} \delta_{n'_2, n_2-1} \right] \delta_{n'_1, n_1}, \end{aligned} \quad (68)$$

$$\begin{aligned} \langle n_1, n_2, \downarrow | \frac{\hbar}{\lambda} \mathcal{H}_{SO} | n'_1, n'_2, \uparrow \rangle = & r_1 \left[(n'_1 + 1)^{1/2} \delta_{n_1, n'_1+1} + n_1^{1/2} \delta_{n_1, n'_1-1} \right] \delta_{n_2, n'_2} \\ & + ir_2 \left[(n'_2 + 1)^{1/2} \delta_{n_2, n'_2+1} + n_2^{1/2} \delta_{n_2, n'_2-1} \right] \delta_{n_1, n'_1} \\ & - f_1 \left[(n'_1 + 1)^{1/2} \delta_{n_1, n'_1+1} - n_1^{1/2} \delta_{n_1, n'_1-1} \right] \delta_{n_2, n'_2} \\ & + if_2 \left[(n'_2 + 1)^{1/2} \delta_{n_2, n'_2+1} - n_2^{1/2} \delta_{n_2, n'_2-1} \right] \delta_{n_1, n'_1} \\ = & \langle n'_1, n'_2, \uparrow | \frac{\hbar}{\lambda} \mathcal{H}_{SO} | n_1, n_2, \downarrow \rangle^*, \end{aligned} \quad (69)$$

from which the hermicity of the spin-orbit term is also apparent.

Evidently, the exact eigenenergies of the Hamiltonian including the Zeeman effect and Rashba spin-orbit coupling are the eigenvalues of a matrix of infinite dimension. This matrix has the Hamiltonian of the anisotropic confinement potential and the orbital effects of the magnetic field as well as the Zeeman term on the diagonal, while the SO (spin-orbit) term determines the entries in the off-diagonal blocks. Specifically,

$$\mathcal{H} = \begin{pmatrix} \left[\sum_{i=1,2} (n_i + \frac{1}{2}) \hbar \omega'_i + \hbar \omega_1 \right] \delta_{n'_1, n_1} \delta_{n'_2, n_2} & \langle n_1, n_2, \downarrow | \frac{\hbar}{\lambda} \mathcal{H}_{SO} | n'_1, n'_2, \uparrow \rangle^* \\ \langle n_1, n_2, \downarrow | \frac{\hbar}{\lambda} \mathcal{H}_{SO} | n'_1, n'_2, \uparrow \rangle & \left[\sum_{i=1,2} (n_i + \frac{1}{2}) \hbar \omega'_i - \hbar \omega_1 \right] \delta_{n'_1, n_1} \delta_{n'_2, n_2} \end{pmatrix} \quad (70)$$

However, we are interested in the behaviour of the low lying energy levels, whose values will have converged if we include a few hundred dimensions. In general, such a finite matrix that includes $n_1, n_2 = 0, \dots, N$, $s_z = \uparrow, \downarrow$ will have dimensions of $2(N+1)^2 \times 2(N+1)^2$. For the purpose of illustration, the specific form of the finite Hamiltonian matrix, which includes only $n_1, n_2 = 0, 1$, $s_z = \uparrow, \downarrow$ is presented in Appendix B. The energy levels are found by diagonalizing a finite Hamiltonian matrix of a few hundred dimensions. The results are shown in Figure 9 for a weak spin-orbit coupling, and in Figure 10 for a spin-orbit coupling strength, λ as measured for Au(111) surface states [5]. Additional plots for other coupling strengths are included in Appendix C.

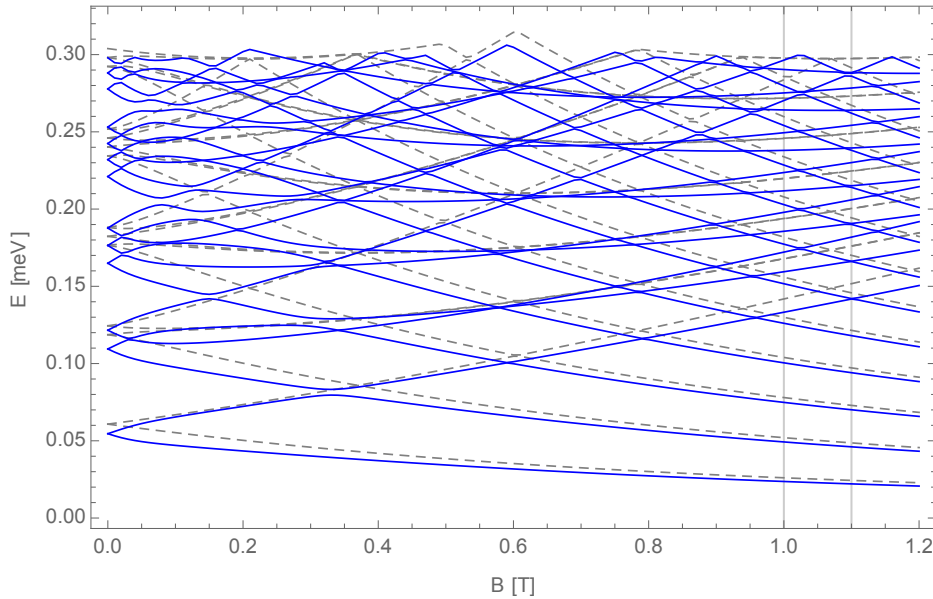


Figure 9: Plot of the low lying energy levels of the anisotropic Fock-Darwin states with Zeeman effect and SO coupling for $\lambda = 0$ (dashed gray lines) and $\lambda = 0.7$ meV nm (blue lines). Energy levels are shown as a function of the magnetic field strength. The vertical lines at $B = 1$ T, 1.1 T mark the values of the confinement potential strengths in the x, y directions such that $\omega_{x,y} = eB_{pot,x,y}/(2m)$.

To distinguish the effect of the Rashba SO coupling on the energy levels, we compare with those of the Fock-Darwin states of an elliptical quantum well with Zeeman effect, which are illustrated in Figure 9 as gray dashed lines. The energy levels including Rashba SO coupling are superimposed on these as blue lines.

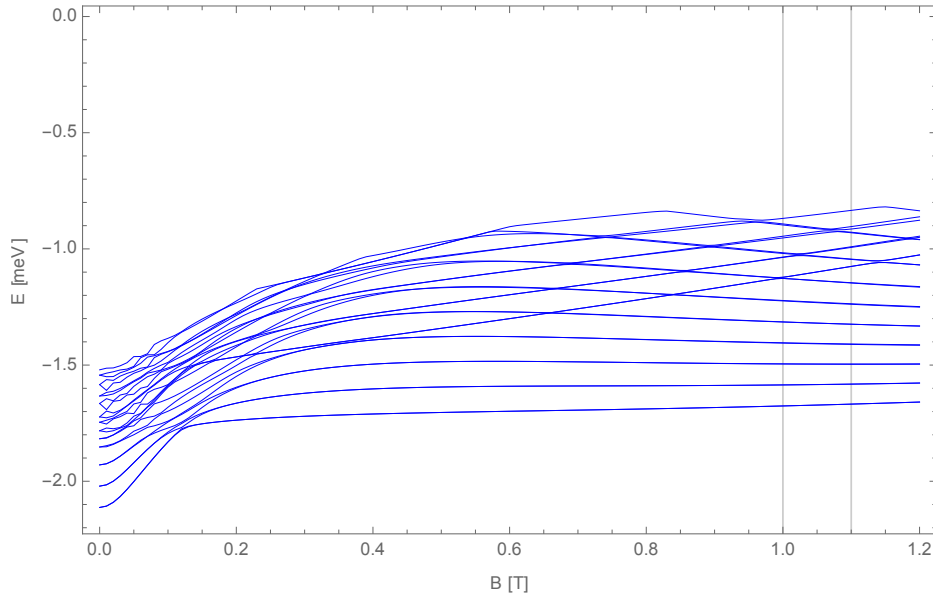


Figure 10: Plot of the low lying energy levels of the anisotropic Fock-Darwin states with Zeeman effect and SO coupling for $\lambda = 35.6$ meV nm and effective electron mass $m_{eff} = 0.250m_e$. Energy levels are shown as a function of the magnetic field strength. The vertical lines at $B = 1$ T, 1.1 T mark the values of the confinement potential strengths in the x, y directions such that $\omega_{x,y} = eB_{potx,y}/(2m)$.

In the limit where $B \rightarrow 0$ the energy levels are doubly degenerate because the system is invariant under time reversal. Because spin-orbit coupling preserves time reversal symmetry the degeneracy is also preserved. Without spin-orbit coupling the energy levels have several crossings, many of which are split as the coupling strength, λ increases from zero. This applies to all crossings between eigenstates of the Hamiltonian for an elliptical quantum well with Zeeman effect that are mixed by the Rashba term. If a state $|n_1, n_2, s_z\rangle$ initially has crossings with $|n_1 + 1, n_2, -s_z\rangle$, $|n_1 - 1, n_2, -s_z\rangle$, $|n_1, n_2 + 1, -s_z\rangle$ or $|n_1, n_2 - 1, -s_z\rangle$ the spin-orbit coupling will split the crossings of these energy levels. If the state $|n_1, n_2, s_z\rangle$ has crossings with any other states than the ones listed above, these crossings will remain. Another effect the spin-orbit coupling has on the spectrum is that it causes the energy levels to form eye-shaped loops when the magnetic field is weak, i.e. a doubly degenerate level at $B = 0$ will split up, initially increasing the spacing between the two levels and subsequently decreasing the spacing until the levels cross. This effect is most pronounced in the plots in Appendix C. The spin-orbit contribution also modifies the energy levels in such a way that they become more negative and spaced further apart. These effects are discernible through a comparison of Figures 9 and 10.

6 Conclusion

We derived an analytical solution for the wave functions and energies of the Landau levels of an electron on a two-dimensional surface with a uniform magnetic field applied perpendicular to its plane of motion. It was shown that the system could be described as a translated harmonic oscillator oscillating at the Larmor frequency with infinitely degenerate energy levels. An analysis was carried out, which concluded that

the degeneracy of each Landau level is reduced to a finite number when the system is placed into a box.

A confinement potential in the form of an isotropic parabolic quantum well was then imposed on the electron moving in two dimensions in a magnetic field. Analytical solutions for the new wave functions and energy levels were derived. The probability densities thus found form circular rings of high probability around the centre of the confinement potential. The probability density currents and magnetic moments produced by the Fock-Darwin states were examined.

The system was analytically solved also for an elliptical confinement potential by transforming the Hamiltonian into that of a two-dimensional harmonic oscillator and working in the creation and annihilation operator formalism. The energy levels were thus known as a function of the parameters of the transformed Hamiltonian, and the ground state could be identified. The Fock-Darwin states in the elliptical confinement potential form elliptical rings of high probability density around the centre of the confinement potential, some with a slightly higher probability on these rings close to either the x- or y-axis depending on the quantum numbers of the state. The probability density currents produced by the Fock-Darwin states in the elliptical well were also examined and compared to those of the circular well.

Finally, the electron spin was taken into consideration, specifically, by adding a Zeeman term and Rashba spin-orbit coupling to the Hamiltonian with the elliptical confinement potential. The energy levels were found numerically by diagonalizing a finite approximation to the infinite Hamiltonian matrix. It was observed that the spin contributes notable modifications to the energy levels. This includes the splitting of several crossings in the energy spectrum, as well as the formation of eye-shaped loops at weak magnetic fields.

7 References

- [1] AVETISYAN, S. Fock-darwin states of anisotropic quantum dots with rashba spin-orbit coupling. Master's thesis, University of Manitoba, 2014.
- [2] AVETISYAN, S., PIETILÄINEN, P., AND CHAKRABORTY, T. Strong enhancement of rashba spin-orbit coupling with increasing anisotropy in the fock-darwin states of a quantum dot. Phys. Rev. B 85, 153301 (2012).
- [3] DARWIN, C. G. The diamagnetism of the free electron. Math. Proc. Cambridge Philos. Soc. 27, 1 (1931), 86–90.
- [4] FOCK, V. Bemerkung zur quantelung des harmonischen oszillators im magnetfeld. Zeitschrift für Physik 47, 5 (1928), 446–448.
- [5] LASHELL, S., MCDUGALL, B. A., AND JENSEN, E. Spin splitting of an au(111) surface state band observed with angle resolved photoelectron spectroscopy. Phys. Rev. Lett. 77, 16 (1996), 3420–3422.
- [6] MADHAV, A. V., AND CHAKRABORTY, T. Electronic properties of anisotropic quantum dots in a magnetic field. Phys. Rev. B 49, 12 (1994).
- [7] SCHRÖDINGER, E. Quantisierung als eigenwertproblem. Annalen der Physik 384, 4 (1926), 361–376.

Appendices

A Transformation of Variables for an Elliptical Quantum Well

We are interested in discovering a canonical transformation of variables for the Hamiltonian,

$$\mathcal{H} = \frac{1}{2m} [p_x^2 + p_y^2 + \Omega_1^2 x^2 + \Omega_2^2 y^2 + 2m\omega_1 (p_x y - p_y x)]. \quad (71)$$

A transformation of the form

$$\begin{aligned} q_1 &= ax + bp_y & p_2 &= cx + dp_y \\ q_2 &= ey + fp_x & p_1 &= gy + hp_x \end{aligned} \quad (72)$$

where $a, b, c, d, e, f, g, h \in \mathbb{R}$, will in general have $[q_i, p_j] = i\hbar\delta_{ij}$ if the following conditions on the coefficients are met,

$$\begin{aligned} af - be &= 0 & dg - hc &= 0 \\ ah - bg &= 1 & ed - fc &= 1. \end{aligned} \quad (73)$$

It is convenient to parameterize the coefficients by trigonometric functions to satisfy these conditions. One such parameterization is

$$\begin{aligned} q_1 &= \cos \chi x + \chi_2 \sin \chi p_y & p_2 &= -\chi_1 \sin \chi x + \cos \chi p_y \\ q_2 &= \cos \chi y + \chi_2 \sin \chi p_x & p_1 &= -\chi_1 \sin \chi y + \cos \chi p_x, \end{aligned} \quad (74)$$

where $\chi, \chi_1, \chi_2 \in \mathbb{R}$ are free parameters. The above transformation is canonical if

$$\chi_1 \chi_2 = 1. \quad (75)$$

B Finite Hamiltonian Matrix with Zeeman Effect and SO Coupling

The finite Hamiltonian matrix, which includes only $n_1, n_2 = 0, 1$, $s_z = \uparrow, \downarrow$ takes the specific form;

$$\begin{pmatrix} \frac{(\alpha_1\beta_1+\alpha_2\beta_2)\hbar}{2m}+\hbar\omega_1 & 0 & 0 & 0 & 0 & \frac{i\lambda}{\hbar}(f_2+r_2) & \frac{-\lambda}{\hbar}(f_1-r_1) & 0 \\ 0 & \frac{(\alpha_1\beta_1+3\alpha_2\beta_2)\hbar}{2m}+\hbar\omega_1 & 0 & 0 & \frac{-i\lambda}{\hbar}(f_2-r_2) & 0 & 0 & \frac{-\lambda}{\hbar}(f_1-r_1) \\ 0 & 0 & \frac{(3\alpha_1\beta_1+\alpha_2\beta_2)\hbar}{2m}+\hbar\omega_1 & 0 & \frac{\lambda}{\hbar}(f_1+r_1) & 0 & 0 & \frac{i\lambda}{\hbar}(f_2+r_2) \\ 0 & 0 & 0 & \frac{3(\alpha_1\beta_1+\alpha_2\beta_2)\hbar}{2m}+\hbar\omega_1 & 0 & \frac{\lambda}{\hbar}(f_1+r_1) & \frac{-i\lambda}{\hbar}(f_2-r_2) & 0 \\ 0 & \frac{i\lambda}{\hbar}(f_2-r_2) & \frac{\lambda}{\hbar}(f_1+r_1) & 0 & \frac{(\alpha_1\beta_1+\alpha_2\beta_2)\hbar}{2m}-\hbar\omega_1 & 0 & 0 & 0 \\ \frac{-i\lambda}{\hbar}(f_2+r_2) & 0 & 0 & \frac{\lambda}{\hbar}(f_1+r_1) & 0 & \frac{(\alpha_1\beta_1+3\alpha_2\beta_2)\hbar}{2m}-\hbar\omega_1 & 0 & 0 \\ \frac{-\lambda}{\hbar}(f_1-r_1) & 0 & 0 & \frac{i\lambda}{\hbar}(f_2-r_2) & 0 & 0 & \frac{(3\alpha_1\beta_1+\alpha_2\beta_2)\hbar}{2m}-\hbar\omega_1 & 0 \\ 0 & \frac{-\lambda}{\hbar}(f_1-r_1) & \frac{-i\lambda}{\hbar}(f_2+r_2) & 0 & 0 & 0 & 0 & \frac{3(\alpha_1\beta_1+\alpha_2\beta_2)\hbar}{2m}-\hbar\omega_1 \end{pmatrix}$$

The energy levels are found by diagonalizing a corresponding, larger, finite matrix.

C Energy Levels for an Elliptical Quantum Well with Zeeman Effect and SO Coupling

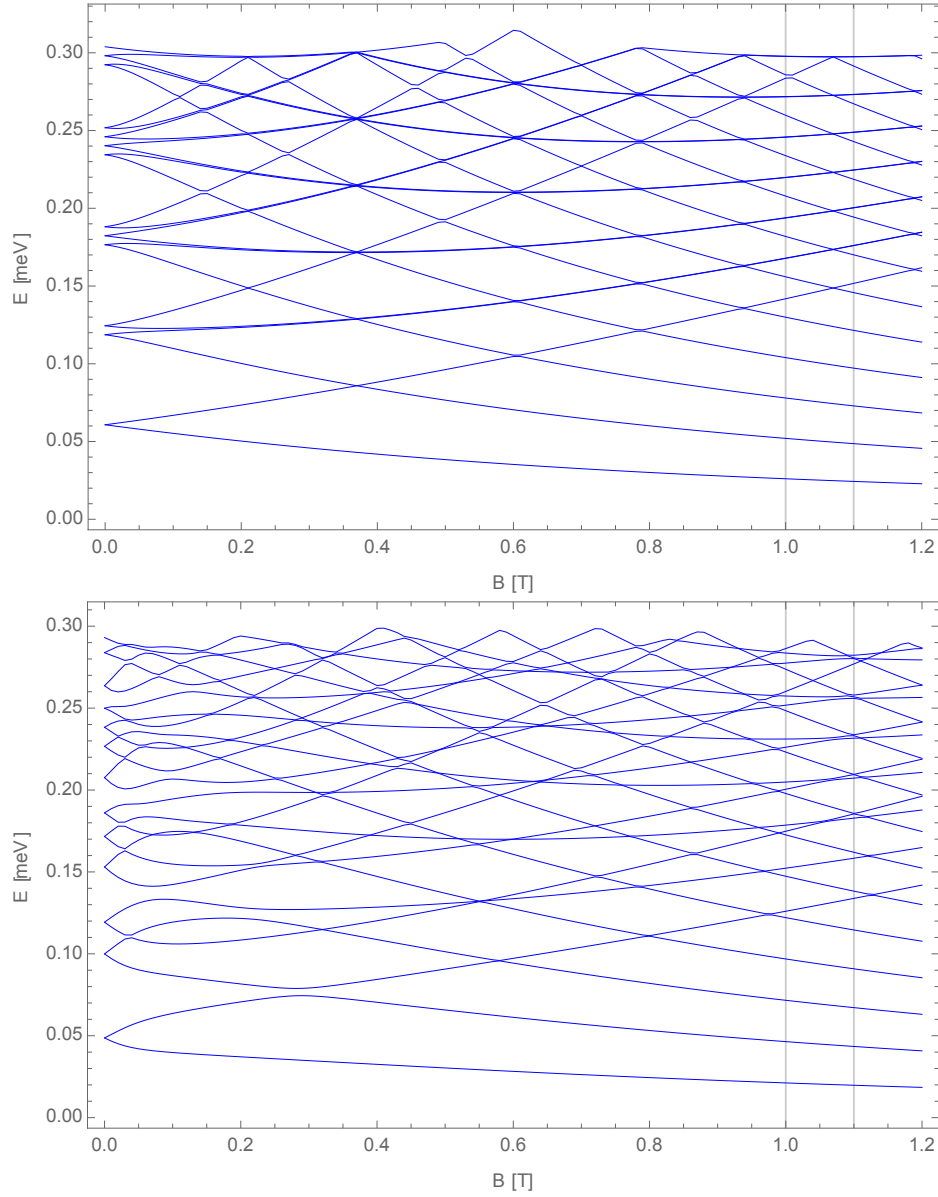


Figure 11: Plots of the low lying energy levels of the anisotropic Fock-Darwin states with Zeeman effect and SO coupling for $\lambda = 0$ (top) and $\lambda = 1$ meV nm (bottom). Energy levels are shown as a function of the magnetic field strength. The vertical lines at $B = 1$ T, 1.1 T mark the values of the confinement potential strengths in the x, y directions such that $\omega_{x,y} = eB_{potx,y}/(2m)$.

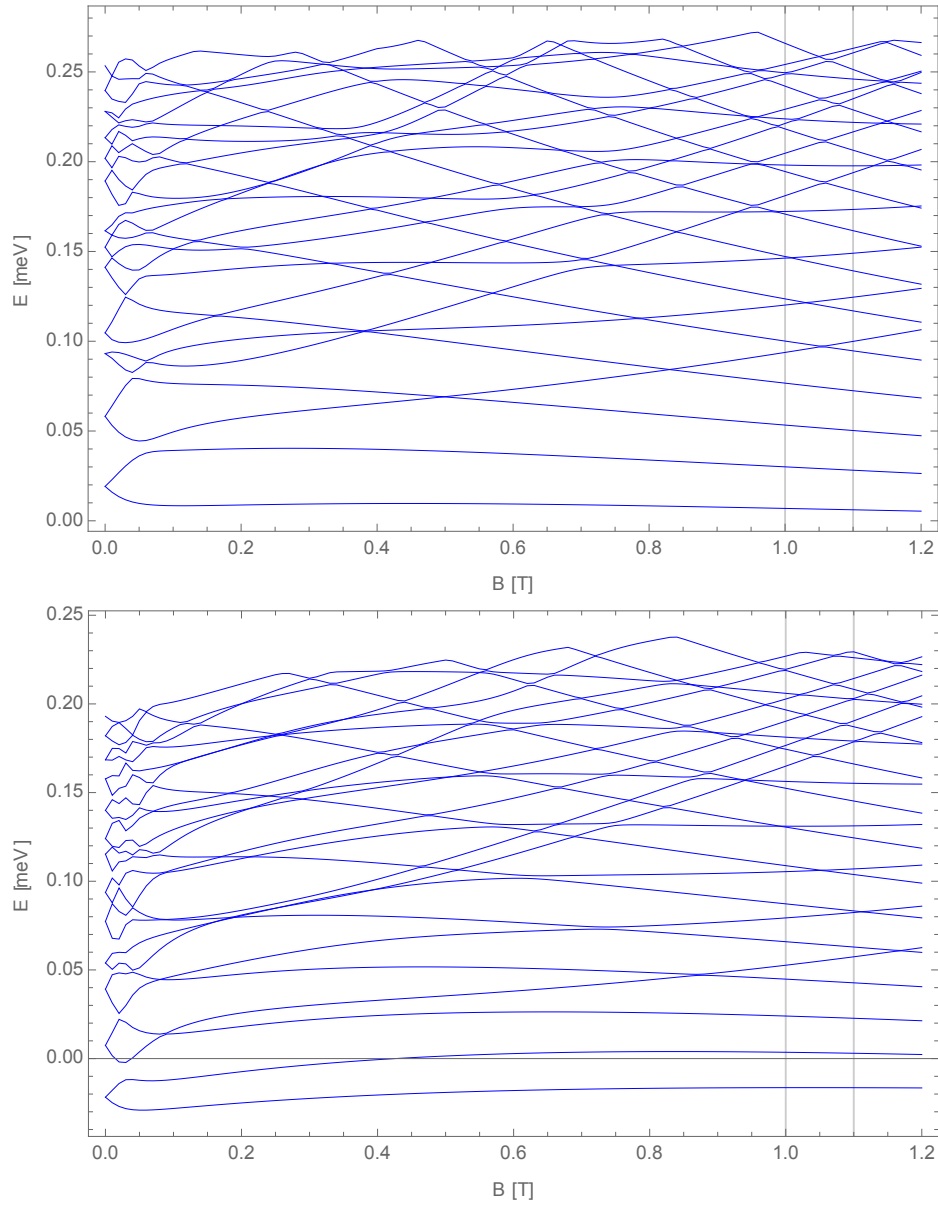


Figure 12: Plots of the low lying energy levels of the anisotropic Fock-Darwin states with Zeeman effect and SO coupling for $\lambda = 2 \text{ meV nm}$ (top) and $\lambda = 3 \text{ meV nm}$ (bottom). Energy levels are shown as a function of the magnetic field strength. The vertical lines at $B = 1 \text{ T}$, 1.1 T mark the values of the confinement potential strengths in the x, y directions such that $\omega_{x,y} = eB_{pot,x,y}/(2m)$.

D Fock-Darwin States for a Circular Quantum Well with Creation and Annihilation Operators

It is of course possible to transform the Hamiltonian for a circular confinement potential (ignoring spin) into a two-dimensional harmonic oscillator in the same manner as with the Hamiltonian for an elliptical confinement potential (the transformation of which was performed in Section 4). This provides an alternative to the analysis carried out in Section 3 for deriving the energy levels and ground state of the Hamiltonian for a circular quantum well.¹

We wish to transform the Hamiltonian,

$$\mathcal{H} = \frac{1}{2m} [p_x^2 + p_y^2 + \Omega^2 (x^2 + y^2) - 2m\omega_1 (xp_y - yp_x)], \quad (76)$$

where

$$\Omega^2 = m^2 (\omega_1^2 + \omega_0^2) \quad (77)$$

to a basis in which it is diagonal. We use the parameterization

$$\begin{aligned} l_1 &= \cos \theta x + \theta_2 \sin \theta p_y & k_2 &= -\theta_1 \sin \theta x + \cos \theta p_y \\ l_2 &= \cos \theta y + \theta_2 \sin \theta p_x & k_1 &= -\theta_1 \sin \theta y + \cos \theta p_x, \end{aligned} \quad (78)$$

which is canonical if

$$\theta_1 \theta_2 = 1. \quad (79)$$

In the new coordinates defined in eqs. (78) the Hamiltonian becomes

$$\begin{aligned} \mathcal{H} &= \frac{k_1^2}{4m} (1 + \theta_2^2 \Omega^2 + \cos 2\theta - \theta_2^2 \Omega^2 \cos 2\theta + 2m\omega_1 \theta_2 \sin 2\theta) + \\ &\frac{k_2^2}{4m} (1 + \theta_2^2 \Omega^2 + \cos 2\theta - \theta_2^2 \Omega^2 \cos 2\theta - 2m\omega_1 \theta_2 \sin 2\theta) + \\ &\frac{l_1^2}{4m} (\theta_1^2 + \Omega^2 - \theta_1^2 \cos 2\theta + \Omega^2 \cos 2\theta + 2m\omega_1 \theta_1 \sin 2\theta) + \\ &\frac{l_2^2}{4m} (\theta_1^2 + \Omega^2 - \theta_1^2 \cos 2\theta + \Omega^2 \cos 2\theta - 2m\omega_1 \theta_1 \sin 2\theta) + \\ &\frac{l_1 k_2}{2m} (-2m\omega_1 \cos 2\theta - \theta_1 \sin 2\theta + \theta_2 \Omega^2 \sin 2\theta) + \\ &\frac{l_2 k_1}{2m} (2m\omega_1 \cos 2\theta - \theta_1 \sin 2\theta + \theta_2 \Omega^2 \sin 2\theta). \end{aligned} \quad (80)$$

By requiring that the coefficients of the off-diagonal terms vanish, we obtain very simple expressions for the transformation parameters,

$$\theta_1^2 = \Omega^2 \qquad \theta = \frac{\pi}{4}. \quad (81)$$

¹In practice this treatment of the Hamiltonian for a circular quantum well served as a sort of prototype for the analysis of the Hamiltonian for an elliptical quantum well.

Thus the transformations in eqs. (78) take the form

$$\begin{aligned} l_1 &= \frac{1}{\sqrt{2}} (x + \Omega^{-1}p_y) & k_2 &= \frac{1}{\sqrt{2}} (-\Omega x + p_y) \\ l_2 &= \frac{1}{\sqrt{2}} (y + \Omega^{-1}p_x) & k_1 &= \frac{1}{\sqrt{2}} (-\Omega y + p_x), \end{aligned} \quad (82)$$

and the Hamiltonian becomes

$$\mathcal{H} = \frac{1}{2m} (\kappa_1^2 k_1^2 + \kappa_2^2 k_2^2 + \epsilon_1^2 l_1^2 + \epsilon_2^2 l_2^2) \quad (83)$$

with

$$\begin{aligned} \kappa_1^2 &= 1 + \frac{m\omega_1}{\Omega} & \kappa_2^2 &= 1 - \frac{m\omega_1}{\Omega}, \\ \epsilon_1^2 &= \Omega^2 \left(1 + \frac{m\omega_1}{\Omega}\right) & \epsilon_2^2 &= \Omega^2 \left(1 - \frac{m\omega_1}{\Omega}\right). \end{aligned} \quad (84)$$

The eigenenergies are then given by

$$E_{n_1, n_2} = \left(n_1 + \frac{1}{2}\right) \hbar\omega_1'' + \left(n_2 + \frac{1}{2}\right) \hbar\omega_2'', \quad n_1, n_2 = 0, 1, \dots \quad (85)$$

where

$$\omega_1'' = \frac{\Omega}{m} \left(1 + \frac{m\omega_1}{\Omega}\right), \quad (86)$$

$$\omega_2'' = \frac{\Omega}{m} \left(1 - \frac{m\omega_1}{\Omega}\right), \quad (87)$$

Substituting these expressions in eq. (85) we obtain

$$E_{n_1, n_2} = \hbar\omega_1 [(n_1 + n_2 + 1) / \omega + (n_1 - n_2)]. \quad (88)$$

This result is identical to eq. (45), which we have already deduced reproduces the energy levels found in Section 3 for $n_{1,2} = k + (|n| \pm n)/2$.

We can now construct creation and annihilation operators in (l, k) space:

$$\begin{aligned} a_1' &= \frac{\epsilon_1}{(2m\hbar\omega_1'')^{1/2}} l_1 + i \frac{\kappa_1}{(2m\hbar\omega_1'')^{1/2}} k_1, \\ a_1'^{\dagger} &= \frac{\epsilon_1}{(2m\hbar\omega_1'')^{1/2}} l_1 - i \frac{\kappa_1}{(2m\hbar\omega_1'')^{1/2}} k_1, \\ a_2' &= \frac{\epsilon_2}{(2m\hbar\omega_2'')^{1/2}} l_2 + i \frac{\kappa_2}{(2m\hbar\omega_2'')^{1/2}} k_2, \\ a_2'^{\dagger} &= \frac{\epsilon_2}{(2m\hbar\omega_2'')^{1/2}} l_2 - i \frac{\kappa_2}{(2m\hbar\omega_2'')^{1/2}} k_2, \end{aligned} \quad (89)$$

in terms of which the Hamiltonian eq. (83) can be written

$$\mathcal{H} = (a_1'^{\dagger} a_1' + \frac{1}{2}) \hbar\omega_1'' + (a_2'^{\dagger} a_2' + \frac{1}{2}) \hbar\omega_2''. \quad (90)$$

We construct the ground state by requiring that both a_1' and a_2' annihilate it.

$$\begin{aligned} 0 &= \langle x, y | a_1' | 0 \rangle \Rightarrow \\ 0 &= (4m\hbar\omega_1'')^{-1/2} [\epsilon_1(x + \Omega^{-1}p_y) + i\kappa_1(-\Omega y + p_x)] \psi_{00}(x, y). \end{aligned} \quad (91)$$

We write $\psi_{00}(x, y) = \zeta_0(x)\phi_0(y)$ to separate the above equation, which becomes

$$C = \epsilon_1 x + \kappa_1 \hbar \psi_0^{-1} \frac{d\zeta_0}{dx}, \quad (92)$$

$$-C = -i \left(\kappa_1 \Omega y + \epsilon_1 \hbar \Omega^{-1} \phi_0^{-1} \frac{d\phi_0}{dy} \right). \quad (93)$$

The ground state is found by integration of the above equations.

$$\psi_{00}(x, y) \propto \exp \left[-\frac{\Omega}{2\hbar} (x - \epsilon_1^{-1} C)^2 \right] \exp \left[-\frac{\Omega}{2\hbar} (y + i\Omega^{-1} \kappa_1^{-1} C)^2 \right] \quad (94)$$

But a'_2 must also annihilate the ground state.

$$\begin{aligned} 0 &= \langle x, y | a'_2 | 0 \rangle \Rightarrow \\ 0 &= (4m\hbar\omega_1'')^{-1/2} [\epsilon_2(y + \Omega^{-1}p_x) + i\kappa_2(-\Omega x + p_y)] \psi_{00}(x, y). \end{aligned} \quad (95)$$

It is possible to express the above equation in terms of the separation constant C and obtain a constraint on C such that both annihilation operators annihilate the ground state. We obtain the following constraint,

$$0 = ix \left(\frac{\epsilon_1 \epsilon_2}{\Omega \kappa_1} - \kappa_2 \Omega \right) + y \left(\epsilon_2 - \Omega^2 \frac{\kappa_1 \kappa_2}{\epsilon_1} \right) - iC \left(\frac{\epsilon_2}{\kappa_1 \Omega} + \frac{\Omega \kappa_2}{\epsilon_1} \right). \quad (96)$$

The coefficients of x and y vanish and we are left with

$$\begin{aligned} 0 &= -i2C \frac{\sqrt{1 - \frac{m\omega_1}{\Omega}}}{\sqrt{1 + \frac{m\omega_1}{\Omega}}} \Rightarrow \\ 0 &= C. \end{aligned} \quad (97)$$

Hence the ground state is

$$\psi_{00}(x, y) = A_0 \exp \left[-\frac{\Omega}{2\hbar} (x^2 + y^2) \right], \quad (98)$$

which correctly reproduces the ground state of the wave functions eq. (25) found in Section 3.